Electro-optical 1 x 2, 1 x N and N x N fiber-optic and free-space switching over 1.55 to 3.0 μm using a Ge-$Ge_2Sb_2Te_5$-Ge prism structure

Joshua Hendrickson,[1,*] Richard Soref,[2] Julian Sweet,[1,3] and Arka Majumdar[4]

[1]*Air Force Research Laboratory, Sensors Directorate, Wright-Patterson Air Force Base, Ohio, 45433, USA*
[2]*Physics Department and the Engineering Program, University of Massachusetts at Boston, Boston, MA 02125 USA*
[3]*Wyle Laboratories, Beavercreek, Ohio 45431 USA*
[4]*Department of Electrical Engineering, University of Washington, Seattle, WA-98195, USA*
**joshua.hendrickson.4@us.af.mil*

Abstract: New device designs are proposed and theoretical simulations are performed on electro-optical routing switches in which light beams enter and exit the device either from free space or from lensed fibers. The active medium is a ~100 nm layer of phase change material ($Ge_2Sb_2Te_5$ or GeTe) that is electrically "triggered" to change its phase, giving "self-holding" behavior in each of two phases. Electrical current is supplied to that film by a pair of transparent highly doped conducting Ge prisms on both sides of the layer. For S-polarized light incident at ~80° on the film, a three-layer Fabry-Perot analysis, including dielectric loss, predicts good 1 x 2 and 2 x 2 switch performance at infrared wavelengths of 1.55, 2.1 and 3.0 μm, although the performance at 1.55 μm is degraded by material loss and prism mismatch. Proposals for in-plane and volumetric 1 x 4 and 4 x 4 switches are also presented. An unpolarized 1 x 2 switch projects good performance at mid infrared.

OCIS codes: (250.6715) Switching; (230.2090) Electro-optical devices; (310.6845) Thin film devices and applications; (060.6719) Switching, packet.

References and links

1. P. Hosseini, C. D. Wright, and H. Bhaskaran, "An optoelectronic framework enabled by low-dimensional phase-change films," Nature **511**(7508), 206–211 (2014).
2. L. Perniola, V. Sousa, A. Fantini, E. Arbaoui, A. Bastard, M. Armand, A. Fargeix, C. Jahan, J.-F. Nodin, A. Persico, D. Blachier, A. Toffoli, S. Loubriat, E. Gourvest, G. B. Beneventi, H. Feldis, S. Maitrejean, S. Lhostis, A. Roule, O. Cueto, G. Reimbold, L. Poupinet, T. Billon, B. De Salvo, D. Bensahel, P. Mazoyer, R. Annunziata, P. Zuliani, and F. Boulanger, "Electrical behavior of phase-change memory cells based on GeTe," IEEE Electron Device Lett. **31**(5), 488–490 (2010).
3. G. Navarro, A. Persico, E. Henaff, F. Aussenac, P. Noe, C. Jahan, L. Perniola, V. Sousa, E. Vianello, and B. DeSalvo, "Electrical performances of SiO_2-doped GeTe for phase-change memory applications," IEEE International Reliability Physics Symposium, Anaheim, CA (14 April 2013).
4. H. T. Kim, B. J. Kim, S. Choi, B. G. Chae, Y. W. Lee, T. Driscoll, M. M. Qazilbash, and D. N. Basov, "Electrical oscillations induced by the metal-insulator transition in VO_2," J. Appl. Phys. **107**(2), 023702 (2010).
5. H. Liang, R. Soref, J. Mu, A. Majumdar, X. Li, and W. P. Huang, "Simulation of silicon-on-insulator channel-waveguide electro-optical modulators and switches using a $Ge_2Sb_2Te_5$ self-holding layer," J. Lightwave Technol. (to be published).
6. R. A. Soref, D. L. McDaniel, and B. R. Bennett, "Guided-Wave Intensity Modulators using Amplitude and Phase Perturbations," J. Lightwave Technol. **6**(3), 437–444 (1988).
7. R. Soref, "Mid-infrared 2 x 2 electro-optical switching by silicon and germanium three-waveguide and four-waveguide directional couplers using free-carrier injection," Photon. Res. **2**(5), 102–110 (2014).
8. K. Shportko, S. Kremers, M. Woda, D. Lencer, J. Robertson, and M. Wuttig, "Resonant bonding in crystalline phase-change materials," Nat. Mater. **7**(8), 653–658 (2008).
9. T. Moriyama, D. Tanaka, P. Jain, and H. Tsuda, "Low crosstalk design of an optical matrix switch using phase-change material," paper IT4A.4, OSA Integrated Photonics Research Conference, Rio Grande, Puerto Rico (2013).
10. R. A. Soref, "Liquid-Crystal Fiber-Optic Switch," Opt. Lett. **4**(5), 155–157 (1979).

#223023 - $15.00 USD Received 15 Sep 2014; revised 27 Nov 2014; accepted 10 Dec 2014; published 5 Jan 2015

11. R. A. Soref and D. H. McMahon, "Total switching of unpolarized fiber light with a 4-port electro-optic liquid-crystal device," Opt. Lett. **5**(4), 147–149 (1980).
12. M. Nedeljkovic, R. Soref, and G. Z. Mashanovich, "Germanium modulation via the free-carrier plasma dispersion effect," European Optical Society Annual Meeting (EOSAM), session TOM2.SO4, Berlin, Germany (17 Sept 2014).
13. J. Mu, Z. Han, S. Grillianda, A. Melloni, J. Michel, L. C. Kimerling, and A. Agarwal, "Towards ultra-subwavelength optical latches," Appl. Phys. Lett. **103**(4), 043115 (2013).
14. P. Hosseini, C. D. Wright, and H. Bhaskaran, "An optoelectronic framework enabled by low-dimensional phase-change films," Nature **511**(7508), 206–211 (2014).
15. D. Krebs, S. Raoux, C. T. Rettner, G. W. Burr, M. Salinga, and M. Wuttig, "Threshold field of phase change memory materials measured using phase change bridge devices," Appl. Phys. Lett. **95**(8), 082101 (2009).
16. F. L. Pedrotti and L. S. Pedrotti, *Introduction to Optics* (Prentice Hall, 1987).
17. A. Yariv, *Optical Electronics in Modern Communications* (Oxford University Press, 1997).
18. R. A. Soref, "Electrooptic 4x4 matrix switch for multimode fiber-optic systems," Appl. Opt. **21**(8), 1386–1393 (1982).
19. L. Chen, "Silicon photonics 8 x 8 broadband optical switch," paper PM2C.1 presented at the OSA Photonics in Switching Conference, San Diego, CA (13 July 2014).

1. Introduction

Electrical activation of the (reversible) thermal phase change in phase-change materials (PCMs) is an emerging technology relevant to optics. According to recent literature [1–3], the PCMs of GeTe and $Ge_2Sb_2Te_5$ (GST) have exhibited better operational characteristics at room temperature than the PCM VO_2 under electrical control [4]. Within the visible spectrum, experiments on a very thin film of GST sandwiched between transparent conducting ITO layers demonstrated a practical and tunable color filter for free-space light traversing the device [1]. We believe that longer wavelengths also have practical PCM applications as discussed here. GST has considerable electro-optical (EO) device potential in the near and mid infrared because the bandgap of this "semiconductor" is 0.77 eV in its amorphous phase and is 0.48 eV in its fcc rocksalt crystal phase. The corresponding bandgaps of GeTe are somewhat wider at 0.78 and 0.55 eV, respectively.

A recent effort by Liang *et al* [5] showed that a thin film of GST sandwiched between doped semiconductor strips of Si or Ge could serve as an EO waveguide in the 1.3 to 3.0 μm wavelength range. Those proposed structures used the transparency of the Si or Ge as well as the semiconductor's electrical conductivity so that voltage applied across the two semiconductor strips would induce the needed thermal effects within GST (the current-induced Joule heating). This type of three-layer SGS structure is exploited in this paper for free-space EO switching in the near and mid infrared, where S refers to doped semiconductor and G to the PCM film. Prism doping does not add significant optical loss at these wavelengths as discussed in section 4 below. The switches offer a unique advantage because the devices are self-holding (for long duration) in each state. Electrical energy is provided only for state transition. Another fundamental advantage is the absence of optical absorption loss in the PCMs at 1.8 - 3.0 μm wavelengths. Let us denote the complex indices of the PCM as $n_{am} + i\ k_{am}$ (for the amorphous phase) and $n_{cr} + i_{cr}$ (for the crystalline phase). The semiconductor-prism's index n_s is carefully matched to n_{am} to provide very high optical transmission in the amorphous state. To attain n_s in the range of 3.85 to 4.15 we selected three group IV prism materials: Ge-rich SiGe for n_s ~3.85, Ge for n_s of 4.05 – 4.10 and GeSn (having a few percent of Sn) for n_s ~4.15. In the crystalline state, the n_{cr} becomes considerably higher than n_{am}, inducing strong reflection (absent in the amorphous state). This crystalline state reflection is strong for the S-polarization of light and is moderate for the P-polarization due to its Brewster angle behavior. Henceforth in this paper, we use the terms TE and TM to refer to the S and P polarizations, respectively. We have used a classical-optics analysis to quantify the reflection, transmission and absorption of the SGS crystal state. Our work accounts fully for the dielectric loss factor k_{cr} of the crystalline state.

Using prism shaped structures made of semiconductor crystal (or polycrystal), we propose device layouts here for 1 x 2, 1 x N and N x N EO switching of collimated (polarized) free-

#223023 - $15.00 USD Received 15 Sep 2014; revised 27 Nov 2014; accepted 10 Dec 2014; published 5 Jan 2015

space light beams incident upon the device, and we quantify the insertion loss of the switch at 1.55, 2.1, and 3 μm wavelengths. The collimated light devices have immediate fiber optic application. Light emerging from an optical fiber can be collimated by a tiny, cylindrical, graded-index lens contacting the fiber end. Therefore, by contacting these lensed fibers to our structures, we postulate 1 x 2, 1 x N and N x N spatial routing switches for fiber-optic cables.

In the context of fiber-optic networks and optical-wireless systems, EO switches have value for routing light beams among the "client transceivers" present at a particular node of the network. In the digital communication system, the switches are not reconfigured typically at the bit rate: instead the switch operates at a lower speed because it routes a packet of bits or a burst of information. Therefore a reconfiguration speed of 100 ns is practical.

This paper begins with a discussion of optimizing 1 x 2 functionality in a nominally 4-port 2 x 2 device. We then compile from the literature the real and imaginary indices of the PCMs that are used in switch simulations at the wavelengths of 1.55, 2.1, and 3 μm. Next, the basic 2 x 2 design is presented after which the EO-prism response is represented mathematically via a three-layer Fabry-Perot formalism. When light impinges obliquely upon the prism's PCM layer, the "off- normal" FP analysis allows us to determine the reflected, transmitted and absorbed components of the collimated beam. Thereby, the insertion loss (IL) and the crosstalk (CT) of the switch in both its states are predicted. After that, we illustrate how the prism-based structures are constructed to make 1 x N and N x N switches, with such switching being performed all in one plane, or in a multi-plane angled-3D structure. The higher-order switches all rely upon an optical series arrangement, a cascading of 1 x 2 switches. Light is transferred from stage to stage via a local PCM in its amorphous phase. We then quantify how a small mismatch of n_s and n_{am} effects this optical transmission and discuss the two-state switching predictions. High performance is expected in the 2000 to 3000 nm range with reduced performance at 1550 nm due to the presence of sizeable k_{cr} and k_{am} components.

2. The 1 x 2 functionality of four port devices

A 2 x 2 electro-optical spatial routing switch has two optical inputs and two optical outputs; ports labeled 1,2 and 3,4 respectively. Rather than partial switching, complete switching is usually desired. The 2 x 2 goal is to transmit light with low loss from 1 to 3 and from 2 to 4 (the through state) or from 1 to 4 and 2 to 3 (the exchange state). The IL and CT in each state are traceable to the switch's geometric layout and PCM properties.

Although excellent progress has been made in resonant photonic switches, here we will focus on non-resonant structures to determine what can be accomplished in broadband routing. It is noteworthy that the loss factors k_{am} and k_{cr} fall off beyond 1.8 μm in contrast to the traditional free-carrier mechanism of switching where the carrier-induced loss k_{fc} builds up strongly with increasing wavelength into the mid infrared. Experience in free-carrier-injected switches [6,7] gives guidelines for the PCM case. It is found generally that the carrier-injected switch-state has IL due to k_{fc}. Because of that, Soref found [6, 7] that a two-waveguide directional coupler was operated best as an "asymmetrical" 1 x 2 device. This asymmetric approach carries over into the PCM case because here the second state shall always have IL issues. That IL is fundamentally due to the Fresnel equations of optics which say that the reflection in the crystal-state, for realistic incidence angles, will never be above ~90%.

Fortunately, there are many applications in which 1 x 2-functioning PCM devices are valuable. As mentioned, the low-loss first state permits cascading of many devices without penalty, and the loss in the second state is usually taken only once within the cascaded structure.

#223023 - $15.00 USD Received 15 Sep 2014; revised 27 Nov 2014; accepted 10 Dec 2014; published 5 Jan 2015

3. Indices of refraction used in simulations

The wavelength of 2100 nm was selected to connect with the EO waveguides of Liang *et al* [5], while 3000 nm is a wavelength at which both k_{am} and k_{cr} have become essentially negligible. The 1550 nm wavelength is key in the silicon photonics art. Here we have taken the GST indices from the experimental results of Sportko *et al* [8]: 4.60 + i 0.12 (am) and 7.45 + i 1.49 (cr) at 1550 nm, 4.1 + i zero (am) and 6.8 + 0.50 (cr) at 2100 nm, and 4.00 + i zero (am) and 6.3 + i zero (cr). The 4.60 value at 1550 nm was judged "too high" to be matched by transparent semiconductor n_s; thus at this wavelength we turned to GeTe with its 4.22 + i 0.12 (am), 6.81 + i 0.30 (cr) from [9], and here the n_{am} = 4.22 was assumed to be contacted by a transparent doped SiGe structure (containing around 90% Ge) with index n_s = 3.85, entailing a 9.6% index difference. The n_{am} values of 4.1 at 2100 nm and 4.0 were obtained via an eye estimation from the experimental plots [8]. The indices used in subsequent analytical solutions for the various phase change and prism materials are provided in Table 1.

Table 1. Refractive indices of materials

Polarization	λ(nm)	Phase Change Material	n_{am}	n_{cr}	Prism Material	n_s
TE	1550	GeTe	4.22 + i0.12	6.81 + i0.3	SiGe	3.85
TE	2100	GST	4.1 + i0.0	6.85 + i0.5	Ge	4.1
TE	3000	GST	4.0 + i0.0	6.3 + i0.0	Ge	4.0

4. The basic mechanism of 2 x 2 EO switching

Figure 1 presents the side view of the three-layer device in both its free-space and fiber-optic embodiments. The light beams, usually TE-polarized, are obliquely incident upon the GST film (they are grazing), and the physical size of the semiconductor prisms such as the facet height is determined by both the incidence angle and the beam diameter. The PCM layer has a thickness that must be optimized in the presence of two factors; optical interference within this lossy dielectric layer (k_{cr} and k_{am}) and the thermal/electrical environment needed to minimize the applied current. In state 2, in order to maximize the optical signal and to minimize the optical crosstalk, we inserted trial values of the PCM layer thickness into the analysis detailed below in Section 5. Thereby an optimum thickness was found for each wavelength. This optimization led to a PCM thickness in the 100 nm range.

#223023 - $15.00 USD Received 15 Sep 2014; revised 27 Nov 2014; accepted 10 Dec 2014; published 5 Jan 2015

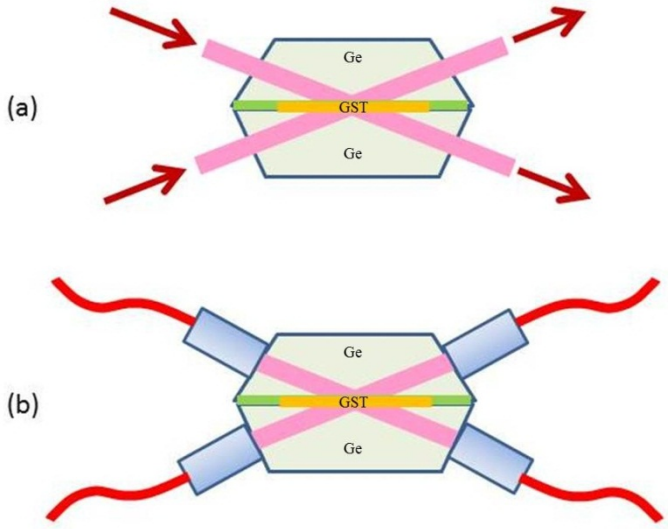

Fig. 1. Schematic view of 2 x 2 EO switch for (a) collimated infrared beams, and (b) optical fibers coupled to Grin-lenses. Prisms are transparent semiconductor doped for conductivity. Active layer is phase-change material. GST refers to this PCM or to GeTe.

Let us first consider TE switching. The idea of this switch is to match the prism index to $n_{am.}$ A second requirement is to have the prism index be much lower than n_{cr}, an index relation that is supplied "automatically" by the PCM. In theory, the match to n_{am} gives 100% transmission in state 1 while the n_{cr}-n_s difference gives high reflection in state 2. It is interesting to compare this mechanism with an alternative EO switching mechanism that was utilized with an alternative EO medium.

The prism structure of Fig. 1 was first presented by Soref [10], where the EO layer between the two prisms was made of nematic liquid crystal (LC) having ordered molecules. In that device, the voltage applied across the two ITO-coated glass prisms produced a dc electric field that re-aligned the LC molecules and changed the LC refractive index that was "felt" by the incoming polarized light beam. In other words, the LC presented either a low index state or a high index state to the polarized light traversing that liquid, where low or high depended upon the E-dependent alignment of the LC. The low index is the ordinary index n_o = 1.492. The high index is the extraordinary index n_e = 1.634. The glass prism index is n_g = 1.644.

The prism-index guidelines in the present PCM switch differ from those in the prior LC switch. For the LC, the switching strategy was to arrange $n_o < n_g \leqq n_e$. And in fact the n_g was chosen to match the "high index" n_e, unlike the PCM case wherein the "low index" n_{am} was matched by n_s. Although our PCM strategy is quite practical, benefits would flow from an alternative strategy similar to that of the LC case (a "supplemental approach" so to speak). However, a transparent conductive prism material with index ~6.8 is not available to match the n_{cr} index, and that's why the alternative approach is not viable. What can be learned from the prior LC EO devices and can be applied here is the geometric layout for cascading the 1 x 2 functions into 1 x N and N x N switching with low loss, in both planar and 3D structures (see section 7 below).

The 1980 LC EO paper of Soref and McMahon [11] reports experiments on simultaneous switching of TE and TM light, termed "total switching of unpolarized light." That was done by means of elongated two-stage prisms that used total internal reflection (TIR) at a glass/air prism interface to transfer the TE and TM light beams from a first EO region to a second, independent EO region. As mentioned above, the LC strategy of matching the prism to the

#223023 - $15.00 USD Received 15 Sep 2014; revised 27 Nov 2014; accepted 10 Dec 2014; published 5 Jan 2015

higher PCM index does not apply here; consequently the 2 x 2 "unpolarized method" of the prior art does not work for the PCM structure. Fortunately, we were able to harness both TE and TM behaviors in a two-stage unpolarized 1 x 2 switch described below.

We shall close this section with a discussion of electroding issues for Fig. 1 devices. In practice, a local region of the high-index prism, a thin volume directly near the PCM, will be doped P type or N type instead of having the entire prism doped. This is illustrated in Fig. 2 where the doped region extends inward from the prism face for just a few micrometers. This near-layer conductivity provides a way to contact the prism electrically with external metallized paths or wires. For example, the two prisms could overlap each other, the top prism overlapping "left" and the bottom prism overlapping "right," and this method would expose two doped Ge areas to the "external world" where the contacts (shown in Fig. 2) could be made. Regarding the optical transmission loss that is introduced by light traveling through the doped electrical-contact region, we would like to highlight the example of N-doped germanium at the wavelength of 2100 nm, assuming a donor concentration of 1 x 10^{18} cm^{-3}. In that case, it is known from Nedeljkovic's calculation [12] that the complex index of Ge is 4.09 + j0.0003 which results in an absorption loss of 0.0078 dB per micron of optical travel through the doped zone. As mentioned above, that transversal is a few microns, therefore, the prism losses are low.

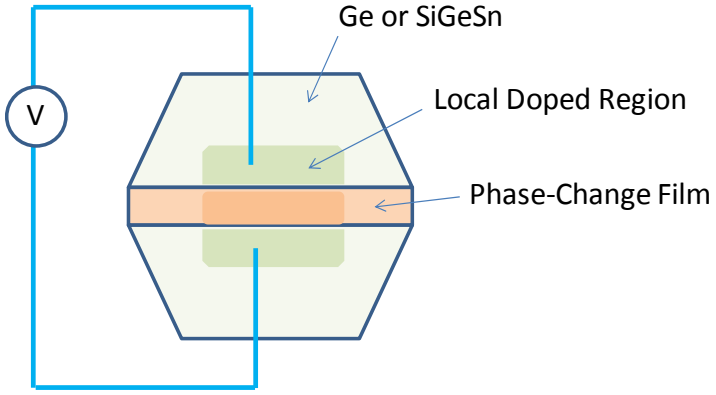

Fig. 2. Details of electrical actuation method for phase-change film.

5. Electrically induced phase change within the prism switch

The electrical conductivity of the N-doped Ge contact regions is more than adequate for good electrical contacts to the GST layer. Specifically, the Ge conductivity at 1 x 10^{18} cm^{-3} doping is 1430 Ohm^{-1} cm^{-1} compared to the crystalline GST conductivity of 277 Ohm^{-1} cm^{-1} [13]. There are reasons to believe that the current injected into GST by voltage pulses applied to the Fig. 2 device is sufficient to induce the desired phase-transition temperature rise in the GST film for films whose thickness is in the range of 62 to 150 nm, as discussed below in section 8. The experimental results of Hosseini *et al.* [14] offers guidelines for the present prism case. Those authors applied a 5V "reset" pulse with duration ~10 ns to a 7-nm GST film sandwiched between ITO electrodes. That voltage was enough to induce the amorphous phase. There, the temperature increased in GST to above the 510°C melting point [14], such as 600°C, and the rapid fall-off of that pulse (< 5 ns) served to freeze the molten material in the am-state. The longer ~100 ns "set" pulse of 2.2 V produced a temperature rise that was above the 155°C crystallization temperature of GST [15], such as 160°C, and this promoted re-crystallization of the film. Regarding the amorphous reset operation, there is experimental evidence that a critical field of 56 V/μm must be reached in the GST film via the applied voltage [15]. This criterion implies a reset voltage of 3.5 V must be applied across a 62 nm

#223023 - $15.00 USD Received 15 Sep 2014; revised 27 Nov 2014; accepted 10 Dec 2014; published 5 Jan 2015

film of GST with 8.4 V of film voltage required at 150 nm of GST. Then, for the associated GST set pulses, the voltages would be lower than these.

6. Analytical equations for 3-layer interference with loss

The EO devices described in this paper are essentially operating as phase change etalons. Therefore, in order to determine the relevant metrics such as reflection, transmission, and absorption we have simply employed the Fabry-Perot equation with reflectivity at the front and back etalon interface found via the Fresnel equations. The Fresnel reflection coefficients for TE and TM incident light at a material interface are given by [16]

$$r_{TE} = \frac{\cos\theta_i - \sqrt{n^2 - \sin^2\theta_i}}{\cos\theta_i + \sqrt{n^2 - \sin^2\theta_i}} \tag{1}$$

$$r_{TM} = \frac{-n^2\cos\theta_i + \sqrt{n^2 - \sin^2\theta_i}}{n^2\cos\theta_i + \sqrt{n^2 - \sin^2\theta_i}} \tag{2}$$

where θ_i is the incident angle and n is the ratio of the complex indices of refraction of material 2 to material 1:

$$n = \frac{\mathrm{n}_2 + \mathrm{ik}_2}{\mathrm{n}_1 + \mathrm{ik}_1} \tag{3}$$

The reflectivity can then be found from:

$$R = rr^* \tag{4}$$

Once the reflectivity values have been calculated they can be substituted into the Fabry Perot equations [17], where the intensity of the reflected signal from an etalon is given as

$$I_r = A_r A_r^* \tag{5}$$

$$A_r = \frac{\left(1 - e^{i\delta}\right)\sqrt{R}}{1 - Re^{i\delta}} \tag{6}$$

the transmission through the etalon is given as

$$I_t = A_t A_t^* \tag{7}$$

$$A_t = \frac{\left(1 - R\right)}{1 - Re^{i\delta}} \tag{8}$$

and the absorption is calculated as

$$I_a = 1 - \left(I_r + I_t\right) \tag{9}$$

with phase delay

$$\delta = \frac{4\pi(\mathrm{n}_2 + \mathrm{ik}_2)l\cos\varphi}{\lambda} \tag{10}$$

#223023 - $15.00 USD Received 15 Sep 2014; revised 27 Nov 2014; accepted 10 Dec 2014; published 5 Jan 2015

In the phase delay equation, l is the etalon thickness, λ is the free space wavelength of light, and φ is the refracted angle within the etalon found from Snell's Law. In the equations above we have assumed unity intensity of the input signal. A schematic diagram of the etalon showing several of the infinite number of reflections and transmissions is presented in Fig. 3.

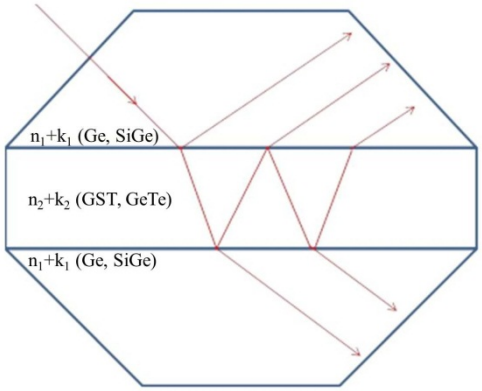

Fig. 3. Illustrating how the two-prism SGS switch may be considered as a Fabry-Perot interferometer for input light incident at an off-normal angle.

7. Results of numerical simulations on switched PCM structures

To numerically characterize our EO devices, the equations from the previous section were all coded in the Python programming language. Starting with a given three-layer SGS material structure and a given wavelength, the reflection, transmission, and absorption were calculated for incident angles spanning 0-90 degrees. The etalon thickness, that is, the PCM layer thickness, was incrementally varied until an optimal size was determined. Those optimum GST and GeTe film thicknesses are listed below.

For the Ge-GST-Ge structure at 2100 nm and 3000 nm, perfect index matching can be obtained when the PCM is in its amorphous state. Since k_{am} is very small in the mid infrared, transmission in this state can be 100%. When the PCM is thermally switched to its crystalline state, the reflectivity, transmission, and absorption will all depend on incidence angle, as shown in Fig. 4. For grazing angles of incidence, the reflection is >80% and transmission is minimal. Complete reflection, transmission and absorption simulations at 2100 and 3000 nm are shown in Fig. 4.

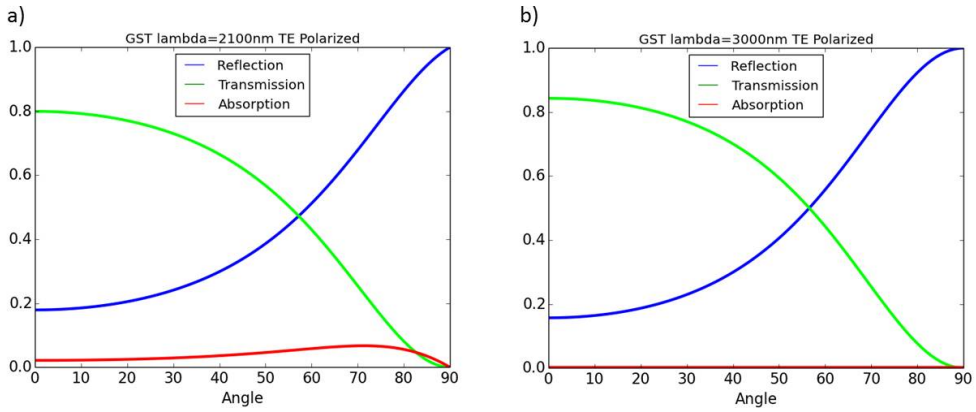

Fig. 4. Reflection, transmission, and absorption as a function of incident angle for (a) Ge-GST-Ge structure at 2100nm and (b) Ge-GST-Ge structure at 3000nm

#223023 - $15.00 USD Received 15 Sep 2014; revised 27 Nov 2014; accepted 10 Dec 2014; published 5 Jan 2015

The SiGe-GeTe-SiGe structure at 1550 nm presents some performance difficulties over the other structures due to the n_{am}-n_s index difference of 0.37; the mismatch between the semiconductor material and the amorphous phase of GeTe. The 1550 nm crystalline state results presented in Fig. 5 are similar in shape but lossier than those curves seen in Fig. 4.

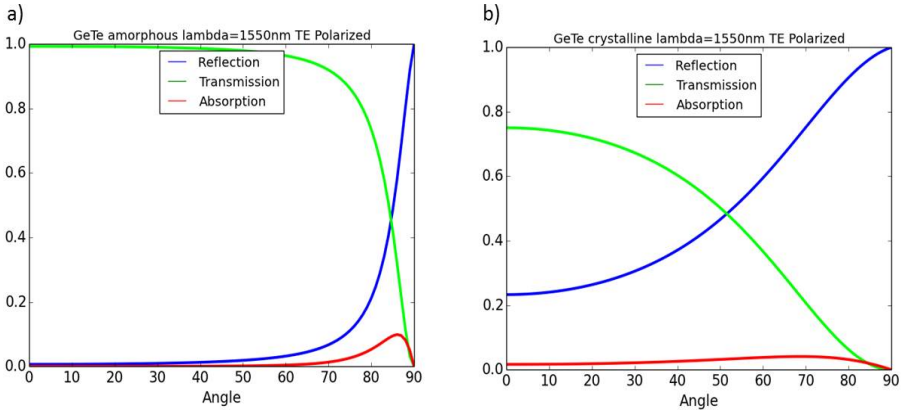

Fig. 5. SiGe-GeTe-SiGe reflection, transmission, and absorption as a function of incident angle for (a) amorphous and (b) crystalline states

Based on the above numerical results, we choose two angles for further analysis: 75 degrees and 80 degrees. The results of all three SGS structures for these chosen angles are discussed below.

It can be a challenge in some cases to attain $n_s = n_{am}$. To quantify the effects of prism/PCM mismatch, we have calculated transmission in the amorphous state for both 1550 and 2100 nm wavelengths, with the results plotted in Fig. 6. This data is needed since n_{am} can be fabrication-dependent. Also, we want to know the improvement gained from better-matching materials. As seen in the 1550 nm case, the n_{am}-n_s ~0.37 degrades the switch performance. Figure 6(b) shows that mismatch-related transmission-loss could arise at 2100 nm. However, at this wavelength, as is indicated in Table 1 above, the match between the semiconductor index and the amorphous index is very close and can be taken as "perfect".

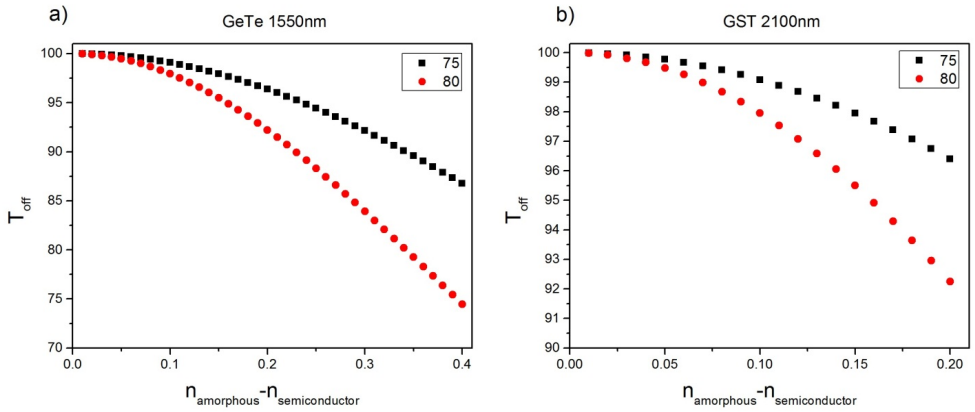

Fig. 6. Transmission for 75 and 80 degree incidence as a function of index mismatch in amorphous state for the (a) SiGe-GeTe-SiGe structure and for the (b) Ge-GST-Ge structure.

8. Discussion of simulation results

Looking at Figs. 4–6, the specific 2 x 2 results at 75 and 80 degrees have been called out and listed in Table 2 along with the optimum film thickness utilized in those figures. We included

#223023 - $15.00 USD Received 15 Sep 2014; revised 27 Nov 2014; accepted 10 Dec 2014; published 5 Jan 2015

the predicted transmission T and reflection R for both the amorphous and crystal phases, and we turned to Fig. 6(a) to determine what the $n_{am} - n_s = 0.37$ caused in T and R for the amorphous phase. For each switch state, it is straightforward to express the Table 2 IL and CT switch performance in decibels: IL(am) = 10 log T, CT(am) = 10 log (R), IL(cr) = 10 log (R), CT(am) = l0 log (T), in which T and R are given in fractions like 0.863 instead of 86.3 per cent.

Table 2. 2 x 2 switch performance metrics at 75 and 80 degrees

λ(nm)	Phase Change Material	Prism Material	t optimal (nm)	Angle (degree)	T_{am}	R_{am}	T_{cr}	R_{cr}
1550	GeTe	SiGe	62	75	86.3	11.1	12.9	83.2
1550	GeTe	SiGe	62	80	73.5	21.2	6.3	90.6
2100	GST	Ge	84	75	100	0	16.3	77.2
2100	GST	Ge	84	80	100	0	8.1	86.3
3000	GST	Ge	150	75	100	0	15.9	84.1
3000	GST	Ge	150	80	100	0	7.7	92.3

Examining the implications of Table 2, the general conclusion is that good 2 x 2 switching (Fig. 1) performance is predicted at 2100 and 3000 nm where the prism-matching gives a very high transmission in state 1. For state 2, the maximum reflection is Fresnel limited as discussed above; nevertheless state 2 is good because here the reflection is above 86% at the larger angle. That reflection ensures very good 1 x 2 functionality because a large percentage is routed in state 2. While the IL of the 2 x 2 at 1550 nm (75° angle) is less than 0.8 dB, the CT is down only 9.2 dB in state 1, which is not as low as the CT at longer wavelengths. The TE switching performance for GeTe at 2100 and 3000 nm is not shown in Table 2. It is known that GeTe has very small k_{am} and k_{cr} in that spectral range, with values of k smaller than the corresponding k of GST cited in Table 1. Therefore, we expect the 2 x 2 signal and crosstalk performance in both state 1 and state 2 to be slightly better than that found for GST in Table 2. Hence we are predicting very good 1 x 2 performance for both GeTe and GST at these "longer" 2 to 3 μm wavelengths.

9. Higher-order EO switching devices

The higher-order routing switches are cascades or interconnections of 1 x 2 devices smoothly joined in minimalistic prism structures. The layout of such prisms is quite analogous to those demonstrated in [18] for the LC case, and three proposals are given here. We are targeting the 2000 to 3000 nm wavelength range, and are predicting that both GeTe and GST will work well. The first design, the 1 x 4 in Fig. 7, is for a TE-polarized input that can travel along the upper prism by a series of TIRs.

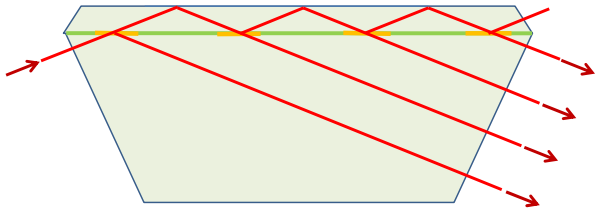

Fig. 7. Side view in cross-section of a 1 x 4 EO Ge/GST/Ge switch.

Four independently addressed local actuation areas of the PCM film are shown and the insertion loss at any of four output ports is expected to be ~1 dB according to Table 1. The second switch, illustrated in Fig. 8, is the 4 x 4 crossbar matrix architecture featuring 16 EO PCM areas provided within a set of 7 parallel PCM films, and having only 4 EO areas actuated into a different phase; that is, twelve areas would be in the amorphous phase and four areas are transitioned to the crystal phase at any time. An interesting aspect of Figs. 7

#223023 - $15.00 USD Received 15 Sep 2014; revised 27 Nov 2014; accepted 10 Dec 2014; published 5 Jan 2015

and 8 is that the switching occurs in just one plane. However, during prism construction it is quite easy to extend the prism material in a direction perpendicular to this page, which means that many switching planes could be deployed in the same set of prisms for simultaneous switching in different planes. For example, in Fig. 7 we could replicate the 1 x 4 six times in the perpendicular direction. This is illustrated in Fig. 5 of [18]. Similarly, the Fig. 8 crossbar could be replicated several times in those prisms in planes parallel to each other.

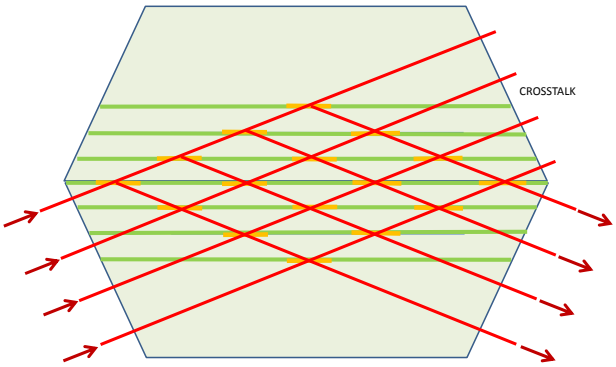

Fig. 8. Side view in cross-section of a 4 x 4 EO Ge/GST/Ge crossbar switch employing 7 GST layers and 8 Ge prism structures, with nonblocking switching in one plane.

We discussed in Fig. 2 above the localized doping and the left-and-right overlap of prisms. This technique applies to both the 1 x 4 and the 4 x 4 switches for electrical contacting. There are no metallized paths that touch the PCM and attenuate the light. The localized doping paths fan out laterally to the exposed overlapped areas of the prisms where electrical contacts are made.

As Chen has pointed out [15], the crossbar is just one of several N x N architectures. He favors the switch-and-select (S&S) architecture shown in Fig. 2(a) of [19]. It turns out that this S&S switch can be implemented in our PCM technology using two prism sets, the first set feeding lightbeams to the second set at a 90° rotation angle, with a thin-film halfwave plate (polarization rotator) interposed in the case of TE-polarized inputs to the N x N. In fact, this switch-and-select device was built and tested years ago for the LC case [18], and we are presenting here an artist's rendering of this 4 x 4 switch-and-select, which by the way can be used in wavelength-division-multiplexed photonic systems if the MUX and DEMUX units are placed, respectively, in front of and behind the 4 x 4. This nonblocking switch can be thought of a four-fold 1 x 4 (Fig. 7) sending its 16 outputs to the 16 inputs of a four-fold 4 x 1 device (Fig. 7). So the Fig. 9 device is a volumetric, angled, 3D structure.

#223023 - $15.00 USD Received 15 Sep 2014; revised 27 Nov 2014; accepted 10 Dec 2014; published 5 Jan 2015

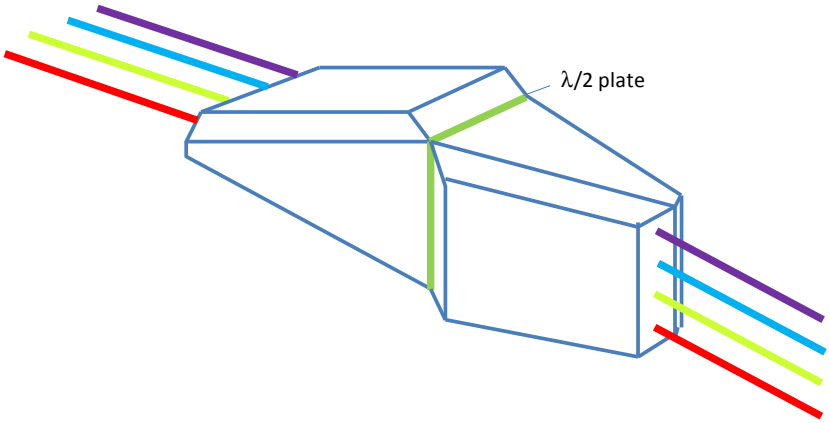

Fig. 9. Perspective view of 4 x 4 EO switch comprised of two joined SGS prism sets: 4(1x4) sending its outputs to 4(4x1). The input collimated light beams are S-polarized.

Our final example is a 1 x 2 switch for unpolarized input light, the configuration presented in Fig. 10. Here the input is comprised of TE and TM components and each polarization can be traced separately as it travels through the prism structure. As in previous switches there are independent EO areas (two areas) and one TIR transfer of TE + TM. A good illustration of the 1 x 2 operation is the GST device functioning at 80° incidence at the 3 μm wavelength. To quantify the IL and CT, we need knowledge of the TM transmission and reflection in both am and cr states. We have done those TM simulations and have found T(am) = 100, R(am) = 0, T(cr) = 38.9 and R(cr) = 61.1. The corresponding TE results are seen in Table 2. For unity input power, unpolarized light (conceptually light with half of its power in TE and with half in TM) the unpolarized outputs (signal and crosstalk) at the first and second output ports of Fig. 10 have been estimated for its two switching states using the foregoing TE and TM data, and our findings are that 100% appears as port-a signal and 0% as port-b crosstalk in state 1 and that there is 76.7% of port-a signal and 8.3% of port-b crosstalk in state 2, which is fairly good performance but not exceptional. Regarding the cr-state, state 2 in Fig. 10, note that 15% of the optical energy is shunted out to the unlabeled upper output port.

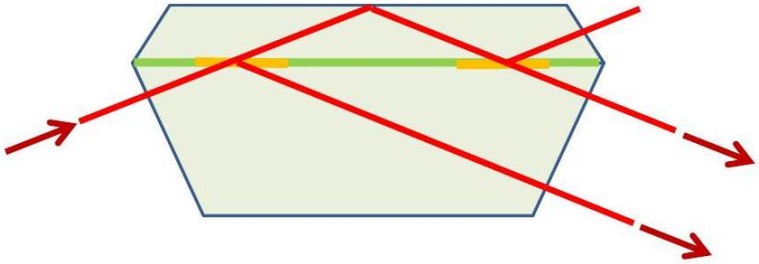

Fig. 10. Side view in cross section of a 1 x 2 EO Ge/GST/Ge switch intended to switch an unpolarized light beam entering the device.

10. GST switching compared to LC switching

In this section, we compare the estimated performance of our 2 x 2, 1 x 4 and 4 x 4 switches with the experimentally measured performance of the corresponding LC prism devices in [10] and [18]. For each prism device, whether GST or LC, there are unwanted reflection losses between the prism material and the surrounding air at the optical inputs and outputs. It is well known in the optical art that those losses can be reduced sharply by applying a thin-film of anti-reflection dielectric at the input and output prism faces. Therefore, we shall not include those losses in the discussion of insertion loss IL and crosstalk CT in the switches. Nor are

#223023 - $15.00 USD Received 15 Sep 2014; revised 27 Nov 2014; accepted 10 Dec 2014; published 5 Jan 2015

such losses included in Table 2 above. A general feature of LC switches is that they are self-holding in the voltage-off state because of wall-induced molecular alignment. However, a holding or sustaining voltage is required to maintain the LC alignment in the voltage-on switching state. By comparison, the GST switch is self-holding in both of its states.

Beginning with the LC 2 x 2 switch [10], a 6 μm layer of nematic LC was used, together with prisms having a 67° angle. An AC voltage of 25 Volts RMS produced complete switching at the 633-nm wavelength. The 2 x 2 LC TM measurements in [10] show that IL = −0.18 dB and CT = −54 dB with voltage off, while the voltage-on state attained IL = −0.6 dB and CT = −11.5 dB. For GST, the key IL and CT parameters of our switch are expressed in our Table 2 as the percent of T and R which we have converted to dB as explained in section 6 above. For comparison with LC, let's look at the 80°-prism TE GST device in Table 2 at the 2100 nm wavelength. Here the (amorphous) first state has a nominal zero IL and an ultra-low CT, whereas in the (crystal) second state IL = −1.1 dB and CT = −10.9 dB. The LC rise and fall times of switches are listed as several milliseconds. By comparison, the set and reset reconfiguration times of our phase-change switches are ~100 ns and ~10 ns, respectively.

Turning now to the 633-nm 1 x 4 LC device of [18], it had a nematic LC layer of 6.3 μm thickness between glass prisms having a 66° angle, together with localized ITO films for four-element "pixel" control. As mentioned, each of four switched areas required a holding-on voltage. For switching on, an AC voltage of 35 Volts RMS was required. The optical IL and CT in the voltage-off state were not cited but are believed to be similar to those in the above-discussed 2 x 2 LC device. The reflection and transmission in the voltage-on state had some variability across the four pixels because of fabrication errors. Those four switched LC transmissions ranged from 70 to 90%; giving IL of −1.55 to −0.46 dB and CT of −5.3 to −10.0 dB. The 1 x 4 LC turn-on time was 1.3 msec, and its fall time was 4.0 msec. The GST has much shorter switching times as mentioned A complete simulation of our Fig. 7 2100 nm 80° GST 1 x 4 switch is beyond the scope of this paper because the strength of the signal and the strength of the crosstalk at each of four possible outputs is different; those four ports have different performance. We can quantify this variation by saying that the IL is expected to range from "zero" dB to 2.2 dB and that the CT is expected to range from a very low value to −10.9 dB. This non-uniformity of performance at the four output ports shows up also in the 4 x 4 switch of Fig. 9, the simulation of which is again outside the scope of this paper..

For the Fig. 8 4 x 4 switch, the "ideal" performance of the am-state at 2 to 3 μm wavelengths is very helpful, and in this "matrix switch" it is seen that the cr-state is used only once in each input-to-output path. Also the crosstalk is shunted away to the upper prisms. For those reasons, our simulation indicates that we would expect −1.1 dB IL and very low CT at all four outputs, irrespective of input choice, that is, uniform performance, for the 80° 2100 nm case. Of course in practice the am-state would deviate from the 100/0 ideality in Table 2, and that deviation would reduce the performance. In summary, the GST switches are judged as more practical than LC in switching speed and self-holding. The GST may also offer lower control voltages but that remains for experimental confirmation. GST switches generally consume less energy than the LC switches.

As a final comment on GST 2 x 2 switching, we turn to the 2 x 2 switch modeling of [5] where a two-state SOI electro-optic GST waveguide segment was embedded in a waveguided switch geometry That GST enabled 2 x 2 switching in a Mach-Zehnder interferometer (MZI) and in a two-waveguide directional coupler (2W). Estimates of TM-polarized IL and CT at the 2100-nm wavelength were made as follows [5]: the MZI with active length of 38 μm had IL(am) = −0.5 dB, CT(am) = −15 dB, IL(cr) = −1.1 dB, CT(am) = −16 dB; whereas the 2W with 67 μm active length had IL(am) = −0.8 dB, CT(am) = −15 dB, IL(cr) = −0.4 dB, CT(am) = −22 dB.

#223023 - $15.00 USD Received 15 Sep 2014; revised 27 Nov 2014; accepted 10 Dec 2014; published 5 Jan 2015

11. Conclusion

One or more thin films of phase change material such as GST or GeTe can form the basis of two-state electro-optical switches for routing collimated light beams in "space" as specified here. The PCM film is self-holding and will stay "indefinitely" in one phase (without input energy) until it is induced electrically to transform into the other phase; a fast, reversible process. The mid-infrared region from 1.8 to 3 μm is ideal for such PCM switching because the dielectric loss factors of the PCM fall off to essentially negligible values in this range, unlike the free-carrier switching effects where loss increases strongly with wavelength.

In this paper, trapezoidal prism structures of crystal Ge are proposed to route the incident beams at oblique, grazing incidence to the PCM film so that the reflection and transmission of the beam can be controlled electrically by the induced PCM phase: amorphous or rocksalt crystal. The doped Ge prisms are both transparent and conductive, the latter being needed to induce electric "heating current" in the film sandwiched between prism conductors.

We have presented designs, primarily for TE-polarization switching, in 1 x 2, 2 x 2, 1 x N, and N x N (crossbar and switch & select) configurations. Although the 1.55 μm versions have reduced performance, the devices operating over 2 to 3 μm wavelengths are seen as promising because the switch's insertion loss and crosstalk at each of its output ports are quite favorable as has been quantified here using a three-layer Fabry Perot classical-optics formalism.

Acknowledgments

JH and JS would like to acknowledge support from AFOSR under LRIR No. 12RY05COR (Gernot Pomrenke, Program Manager). RS appreciates the financial support of the Air Force Office of Scientific Research under grant FA9550-14-1-0196 (Gernot Pomrenke, Program Manager) of the the UK EPSRC under project MIGRATION. AM is supported by the startup fund provided by the UW-Seattle.